Published in final edited form as:
Nature. ; 485(7400): 661–665. doi:10.1038/nature11066.

AMPK regulates NADPH homeostasis to promote tumour cell survival during energy stress

Sang-Min Jeon[1,†], **Navdeep S. Chandel**[2], and **Nissim Hay**[1]

[1]Department of Biochemistry and Molecular Genetics, College of Medicine, University of Illinois at Chicago, Chicago, Illinois 60607, USA.

[2]Department of Medicine, Division of Pulmonary and Critical Care Medicine, Northwestern University Medical School, Chicago, Illinois 60611, USA.

Abstract

Overcoming metabolic stress is a critical step for solid tumour growth[1,2]. However, the underlying mechanisms of cell death and survival under metabolic stress are not well understood. A key signalling pathway involved in metabolic adaptation is the liver kinase B1 (LKB1)–AMP-activated protein kinase (AMPK) pathway[2,3]. Energy stress conditions that decrease intracellular ATP levels below a certain level promote AMPK activation by LKB1. Previous studies showed that LKB1-deficient or AMPK-deficient cells are resistant to oncogenic transformation and tumorigenesis[4–6], possibly because of the function of AMPK in metabolic adaptation. However, the mechanisms by which AMPK promotes metabolic adaptation in tumour cells are not fully understood. Here we show that AMPK activation, during energy stress, prolongs cell survival by redox regulation. Under these conditions, NADPH generation by the pentose phosphate pathway is impaired, but AMPK induces alternative routes to maintain NADPH and inhibit cell death. The inhibition of the acetyl-CoA carboxylases ACC1 and ACC2 by AMPK maintains NADPH levels by decreasing NADPH consumption in fatty-acid synthesis and increasing NADPH generation by means of fatty-acid oxidation. Knockdown of either ACC1 or ACC2 compensates for AMPK activation and facilitates anchorage-independent growth and solid tumour formation *in vivo*, whereas the activation of ACC1 or ACC2 attenuates these processes. Thus AMPK, in addition to its function in ATP homeostasis, has a key function in NADPH maintenance, which is critical for cancer cell survival under energy stress conditions, such as glucose limitations, anchorage-independent growth and solid tumour formation *in vivo*.

The lack of LKB1 or AMPK activation rendered cancer cells more sensitive to cell death induced by glucose deprivation[5,7–9] (Supplementary Fig. 1). However, the mechanism by which the failure to activate AMPK accelerates cancer cell death during energy stress remains to be explained. Our results demonstrate that the effect of AMPK does not involve p53 or mTORC1, which were implicated in the LKB1–AMPK-mediated regulation of cell survival during glucose deprivation[8,10]. In both control A549 cells (A549-Vect) and dominant-negative p53 (p53DN)-expressing A549 cells (A549-p53DN), LKB1

Correspondence and requests for materials should be addressed to N.H. (nhay@uic.edu).
†Present address: Research Oncology, Genentech, South San Francisco, California 94080, USA.

Supplementary Information is linked to the online version of the paper at www.nature.com/nature.

Author Contributions S.-M.J. and N.H. designed the experiments. S.-M.J. performed the experiments. N.S.C. provided advice. S.-M.J. and N.H. analysed the data and wrote the paper.

reconstitution restored AMPK activation, as measured by ACC phosphorylation, and inhibited glucose-starvation-induced cell death to a similar extent (Fig. 1a, b). mTORC1 inhibition with rapamycin also did not affect the sensitivity of A549 cells to glucose deprivation (Fig. 1b).

Replacement of glucose with the non-metabolizable glucose analogues 2-deoxyglucose (2DG) or 5-thioglucose (5TG) revealed that only 2DG protected LKB1-deficient cancer cells (A549 and HeLa) from glucose-starvation-induced cell death (Fig. 1b and Supplementary Fig. 2b). Unlike 5TG, 2DG strongly induced the activation of AMPK, even in LKB1-deficient cells (Fig. 1a and Supplementary Fig. 2a). This activation occurred by means of a poorly understood mechanism that is dependent on hexokinase (Supplementary Fig. 3). The results suggest that, by activating AMPK, 2DG inhibits cell death during glucose deprivation. However, LKB1 reconstitution in A549 cells induced higher AMPK activation than 2DG (Fig. 1a), yet 2DG protected the cells slightly better than LKB1 (Fig. 1b), implying that 2DG could protect cells by both AMPK-dependent and AMPK-independent mechanisms.

Glucose limitations could induce oxidative stress by decreasing NADPH generation in the pentose phosphate pathway (PPP) (Fig. 1c). NADPH is required for the regeneration of reduced glutathione (GSH), which is used by glutathione peroxidase (GPX) to eliminate H_2O_2 (Fig. 1c). We therefore speculated as follows: first, that the failure to activate AMPK by glucose deprivation accelerates cell death through oxidative stress mediated by decreased PPP flux and NADPH/GSH generation; second, that AMPK activation under these conditions is required to inhibit cell death by decreasing oxidative stress; and third, that 2DG protects the cells by both AMPK activation and partial utilization in the PPP[11] (Fig. 1c).

We first established that decreased PPP flux and increased oxidative stress are the cause of the cell death. Glucose-6-phosphate dehydrogenase (G6PD) knockdown accelerated cell death in low glucose (Fig. 1d) and even in the absence of glucose (Supplementary Fig. 4a, b). Glucose deprivation rapidly depleted NADPH/GSH and elevated the H_2O_2 level in control cells, which were further affected by G6PD knockdown (Supplementary Fig. 4c–e). Finally, the antioxidants *N*-acetylcysteine (NAC) and catalase inhibited cell death in LKB1-deficient or AMPK-deficient cells (Fig. 1e and Supplementary Figs 1c, 5 and 6).

We next examined the function of AMPK in redox regulation by using A549-Vect and A549-LKB1 cells. Unlike A549-Vect cells, A549-LKB1 cells maintained $NADP^+$/NADPH and GSSG/GSH ratios and prevented the increase in the H_2O_2 level during glucose starvation (Fig. 1f, g and Supplementary Fig. 7). Expression of p53DN showed a faster depletion of NADPH and increase in H_2O_2 level (Fig. 1f, g), explaining increased cell death (Fig. 1e). The superoxide (O_2^-) level was not increased (Fig. 1h), suggesting that the increased H_2O_2 level is due to NADPH depletion and impaired H_2O_2 detoxification. LKB1 reconstitution neither decreased the O_2^- level (Fig. 1h) nor changed that of catalase (Fig. 1a), further suggesting that NADPH maintenance is the predominant mechanism by which AMPK prevents oxidative stress. Consistently, LKB1 or AMPKα1 knockdown in MCF7 or H1703 cells significantly increased H_2O_2 levels, but not those of O_2^-, during glucose deprivation (Supplementary Fig. 8). Similarly, AMPKα-knockout (AMPKα-KO) murine embryonic fibroblasts (MEFs) failed to maintain their $NADP^+$/NADPH ratio and low H_2O_2 level after glucose starvation (Fig. 1i). Finally, as we had speculated, 2DG maintained NADPH, GSH and H_2O_2 levels and protected from cell death largely by means of AMPK activation and to a smaller extent by partial utilization in the PPP (Supplementary Fig. 4). This could explain why 2DG protects from cell death slightly better than LKB1 despite higher activation of AMPK by LKB1 (Fig. 1b). Thus, the combination of decreased NADPH generation by the PPP and impaired AMPK activation during glucose deprivation in LKB1-

deficient or AMPK-deficient cells accelerates NADPH depletion and H_2O_2 elevation, eventually causing cell death.

Next we investigated the mechanism by which AMPK maintains the NADPH level in the absence of glucose. The intracellular NADPH level is determined by the difference between its production and its consumption. NADPH is generated from the PPP and mitochondrial metabolism, and is consumed mainly during H_2O_2 detoxification by GPX and peroxiredoxin (PRX) and fatty-acid synthesis (FAS) (Fig. 2a). Under limited glucose supply, the major NADPH source is mitochondrial metabolism, which is supported by fatty-acid oxidation (FAO). Metabolites provided by FAO to the tricarboxylic acid cycle generate malate and citrate, the substrates of NADPH-producing malic enzyme and isocitrate dehydrogenase, respectively. AMPK regulates fatty-acid metabolism through the phosphorylation and inhibition of ACC1 and ACC2, which in turn inhibit FAS and activates FAO, respectively[12]. Both ACC1 and ACC2 generate malonyl-CoA, the precursor of FAS and a potent inhibitor of carnitine palmitoyltransferase 1 (CPT1), the rate-limiting enzyme in FAO[13] (Fig. 2a). We therefore reasoned that AMPK might regulate NADPH homeostasis by inhibiting ACC1 and ACC2.

We first determined whether targeting ACC1 or ACC2 inhibits cell death, the accumulation of H_2O_2 and the depletion of NADPH observed during glucose deprivation. Targeting either ACC1 or ACC2 in A549 cells by short interfering RNAs (siRNAs) demonstrated that only ACC2 knockdown significantly inhibited cell death and H_2O_2 accumulation, without decreasing O_2^- (Supplementary Fig. 9). We therefore generated stable cell lines expressing ACC2-specific short hairpin RNA (shRNA) (Supplementary Fig. 10a). ACC2 knockdown in A549 cells maintained the $NADP^+$/NADPH ratio (Fig. 2b) and the GSSG/GSH ratio (Fig. 2c), inhibited the accumulation of H_2O_2 (Fig. 2d) and prevented cell death (Fig. 2e). Similar results were obtained in HeLa, MCF7-LKB1sh and H1703-LKB1sh cells (Supplementary Fig. 10b–d). Targeting either ACC1 or ACC2 in AMPKα-KO MEFs significantly decreased the H_2O_2 level during glucose starvation (Supplementary Fig. 11). The inability of ACC1 knockdown in A549 cells to decrease the H_2O_2 level during glucose starvation was probably because FAS inhibition in these cells occurs to a similar extent regardless of LKB1 expression or ACC1 knockdown (Supplementary Fig. 12). In contrast, A549-LKB1 and A549-ACC2sh cells showed a marked increase in FAO, explaining why ACC2 knockdown was able to decrease H_2O_2 levels but ACC1 knockdown was not (Supplementary Fig. 12). Consistently, overexpression of the constitutively active ACC2(S212A) mutant significantly inhibited FAO and sensitized MCF7 cells to glucose-deprivation-mediated cell death, and partly blocked protection by 2DG in HeLa cells (Supplementary Fig. 13). Furthermore, short-term exposure to the FAS inhibitor C75, which also activates CPT1, mimicking the effects of AMPK on fatty-acid metabolism, lowered the $NADP^+$/NADPH ratio and protected A549 and HeLa cells during glucose deprivation (Fig. 2b and Supplementary Fig. 14a, b). However, because C75 inhibits FAS downstream of ACC1, long-term treatment with C75 leads to the cytotoxic accumulation of malonyl-CoA[14]. Indeed, etomoxir, a CPT1 inhibitor, abrogated the short-term effect of C75 without affecting the effect of NAC (Supplementary Fig. 14c). These results indicate that the short-term protective effect of C75 was largely due to the activation of CPT1 and the acceleration of FAO. Furthermore, treatment with the ACC inhibitor TOFA protected from cell death, whereas the malate supplement alone could not (Supplementary Fig. 15a). However, the combination of TOFA and malate further protected from cell death (Supplementary Fig. 15a). These results suggest that malate alone is not sufficient to induce NADPH accumulation, because NADPH could still be consumed by FAS. Thus, when FAS is inhibited by TOFA, malate can promote sufficient NADPH accumulation to inhibit cell death during glucose deprivation. Finally, the protective effect of ACC2 knockdown was abrogated by buthionine sulfoximine, which

depletes GSH, but not by nicotinamide (NAM), which inhibits Sirt1, excluding a possible involvement of the NAD^+–Sirt1 pathway[15] (Supplementary Fig. 15b).

Like glucose starvation, matrix detachment elicits energy stress followed by elevated H_2O_2 levels and cell death[16]. Indeed, matrix detachment inhibited glucose uptake in A549 cells (Supplementary Fig. 16), and markedly activated AMPK in A549-LKB1 cells (Fig. 3a). AMPK was also activated in A549 cells but to a much smaller extent than in A549-LKB1 cells (Fig. 3a), which is dependent on calmodulin-dependent protein kinase kinase (CaMKK; Fig. 3b). We therefore tested whether AMPK activation is required for redox regulation during matrix detachment and anchorage-independent growth, which is a hallmark of cancer cells. Matrix detachment significantly increased the H_2O_2 level in A549-Vect cells in comparison with A549-LKB1 cells, regardless of p53 status (Fig. 3c). CaMKK inhibition in A549 cells further elevated the H_2O_2 level during matrix detachment (Fig. 3d), supporting a key function for AMPK in redox regulation during this process. The results were confirmed in MCF7 cells with LKB1 knockdown or AMPKα1 knockdown (Supplementary Fig. 17). The impaired AMPK activation and the higher H_2O_2 level in matrix-detached A549 cells were correlated to the extent of NADPH depletion (Fig. 3e). The high $NADP^+$/NADPH ratio in A549 cells was further increased after matrix detachment, whereas the low $NADP^+$/NADPH ratio was maintained in A549-LKB1 cells (Fig. 3e).

We next investigated whether ACCs mediate the effect of AMPK during matrix detachment. Knockdown of ACC1 by siRNA, but not that of ACC2, blocked the increase in the H_2O_2 level by matrix detachment (Supplementary Fig. 18). We therefore used A549 cells expressing ACC1-specific shRNA (Supplementary Fig. 19) and confirmed that ACC1 knockdown markedly decreased the $NADP^+$/NADPH ratio and H_2O_2 level (Fig. 3f, g). Finally, the ACC inhibitor TOFA, but not the mTORC1 inhibitor rapamycin, decreased the H_2O_2 level (Supplementary Fig. 20). LKB1 expression had a more pronounced effect on FAS inhibition than on FAO increase (Supplementary Fig. 21a). This effect was recapitulated by ACC1 knockdown (Supplementary Fig. 21b), explaining why ACC1 knockdown could decrease the H_2O_2 level.

We then assessed whether redox regulation by ACCs has a function in anchorage-independent growth. Consistent with previous observations[16], we found that treatment of A549 cells and AMPKα-KO-Ras^{V12} MEFs with NAC substantially increased the number of colonies (Fig. 4a and Supplementary Fig. 22). Inhibition of CaMKK markedly inhibited anchorage-independent growth, which was rescued by NAC treatment (Fig. 4a and Supplementary Fig. 22a). Targeting either ACC1 or ACC2 substantially increased the number of colonies on soft agar and recapitulated the effect of NAC (Fig. 4b, c and Supplementary Fig. 23). However, the average colony size was increased only by ACC1 knockdown (Fig. 4b, c), which may reflect the predominant function of ACC1 in controlling the H_2O_2 level after matrix detachment.

To assess further the function of ACCs in anchorage-independent growth, we overexpressed the ACC1(S79A) and ACC2(S212A) mutants in two LKB1-proficient cell lines, MCF7 and H1703. Both mutants increased FAS and the H_2O_2 level after matrix detachment (Fig. 4d and Supplementary Fig. 24a), and potently inhibited anchorage-independent growth, which was partly rescued by NAC (Fig. 4e and Supplementary Fig. 24b, c). These results indicate that the inhibition of either ACC1 or ACC2 by AMPK is required for anchorage-independent growth by means of redox regulation. In contrast, ACC1 knockdown or ACC2 knockdown in LKB1-reconstituted HeLa cells inhibited anchorage-independent growth (Supplementary Fig. 25a). Thus, when AMPK is activated, further inhibition of ACC1 or ACC2 could not enhance tumorigenesis, instead attenuating it.

During the formation of a solid tumour, cells undergo metabolic stress including glucose deprivation and matrix detachment. Indeed, it has been shown that AMPKα-KO-Ras^{V12} MEFs are severely impaired in their ability to form tumours *in vivo*[6] and that AMPK is activated during the early stages of solid tumour formation[17]. Thus, to determine whether ACCs have a function in solid tumour formation *in vivo*, we performed xenograft assays using A549 and AMPKα-KO-Ras^{V12} MEFs expressing shRNAs targeting ACC1 or ACC2. Knockdown of ACC1 or ACC2 significantly enhanced tumour formation *in vivo* (Fig. 4f, g); the latter had a more pronounced effect on tumour growth than the former. However, neither ACC1 knockdown or ACC2 knockdown in A549-LKB1 cells had much effect on tumour growth (Supplementary Fig. 25b), further suggesting that physiological inhibition of ACC by AMPK, but not enhanced inhibition, is required to promote solid tumour growth. To assess these results further, we performed orthotopic transplantation using MCF7 cells. The knockdown of either LKB1 or AMPKα1 in MCF7 cells significantly inhibited orthotopic tumour growth (Supplementary Fig. 26a). To test the function of ACC1 and ACC2 phosphorylation by AMPK in tumour growth, MCF7 cells expressing either ACC1(S79A) or ACC2(S212A) were subjected to orthotopic transplantation. Consistent with the *in vitro* results (Fig. 4e), ACC2(S212A) expression significantly inhibited solid tumour growth; ACC1(S79A) expression also inhibited tumour growth, although to a smaller extent, under two different experimental conditions (Fig. 4h and Supplementary Fig. 26b). Taken together, these results demonstrate that NADPH maintenance through AMPK–ACC1/ACC2 is critical for solid tumour growth *in vivo* (Fig. 4i). It was previously reported that ACC2 expression is significantly downregulated in papillary thyroid cancer[18], supporting a tumour-suppressor function for ACC2 in certain contexts. Moreover, consistent with our results, it was shown that overexpression of CPT1 promotes solid tumour growth through the activation of FAO[19].

Our results are not inconsistent with results showing that inhibition of FAS by the knockdown of fatty acid synthase (FASN) or ATP-citrate lyase (ACLY) inhibits tumorigenesis[20,21] because, unlike the inhibition of ACC, the inhibition of FASN or ACLY exerts additional cytotoxic effects. These cytotoxic effects seem to be through the accumulation of malonyl-CoA but not through the direct inhibition of FAS itself[14,22,23], and through the inhibition of acetylation without decreasing lipid contents[24,25]. Our results seem paradoxical because of the tumour suppressor activity of LKB1–AMPK, partly through mTORC1 inhibition[3]. We propose that during glucose limitations or matrix depletion, AMPK activation, at physiological levels, is required for NADPH homeostasis, which surpasses the requirement for mTORC1 activity. Combating energy stress conditions by AMPK is particularly important in the early stages of solid tumour formation when cells migrate to the lumen, or during metastasis when cells migrate from the primary tumour to a different location. However, AMPK activation is probably occurring in a temporal manner, because FAO could also increase the ATP level (Supplementary Fig. 27), which would eventually inhibit AMPK. Our results therefore do not necessarily contradict the possibility that prolonged and robust AMPK activation inhibits cancer cell proliferation. In fact, they suggest that a combination of metabolic inhibitors, such as 2DG or metformin, and ACC activators could synergistically decrease cancer cell survival by concurrently inhibiting mTORC1 and the pro-survival activity of AMPK. This combination could be more effective in LKB1-null cancer cells.

Our findings could explain why AMPK-deficient cells are resistant to oncogenic transformation[4,6]. At the organismal level our results may explain why patients with Peutz–Jeghers syndrome, who have an inherited deficiency of LKB1, and most mouse models of LKB1 deficiency develop only benign tumours[4]. Although somatic mutations in LKB1 are rare in most cancers, the mutations are prevalent in certain cancers, such as non-small cell lung carcinoma and cervical carcinoma[3]. In mouse models, deficiency in LKB1 also

promotes Ras-induced lung tumorigenesis[26]. One possible explanation is that certain microenvironmental factors may enable AMPK activation in the absence of LKB1 through other upstream activators, such as CaMKK, as shown in Fig. 3b. In addition, LKB1 deficiency may affect other multiple downstream effectors of LKB1 (ref. 26) that could circumvent the requirement for the LKB1–AMPK pathway during the early stages of solid tumour formation.

AMPK is known to maintain intracellular ATP level under conditions of energy stress. Consistently, we found that AMPK maintains ATP level in addition to NADPH level under these conditions (Supplementary Fig. 27a). However, NAC, which protected from cell death, did not restore ATP level during glucose starvation (Supplementary Fig. 27b), indicating that NADPH maintenance rather than ATP maintenance is the predominant mechanism by which AMPK promotes cell survival during metabolic stress (Fig. 4j).

Our study shows that under conditions of energy stress, when NADPH generation from the PPP is impaired, AMPK activation is required for the maintenance of NADPH level by inhibiting ACC1 and/or ACC2 (Fig. 4i, j). This function of AMPK is critical for cancer cell survival during metabolic stress, which can occur in the solid tumour microenvironment.

METHODS

Cell culture, transfection, transduction and western blotting

MI5-4 CHO cells (a gift from J. Willson) were cultured in α-MEM supplemented with 2 mM glutamine and 10% FBS (Gemini). All other cells were cultured in DMEM (Invitrogen) containing 10% FBS. For the glucose starvation experiments, the cells were washed with PBS and cultured in glucose-free DMEM(Invitrogen) containing 10% dialysed FBS (Gemini). For suspension culture, the cells were plated on poly-HEMA (2-hydroxyethyl methacrylate)-coated plates. For the transient transfection of the siRNAs, 2×10^5 A549 cells or 10^5 AMPKα1/α2-DKO MEFs immortalized with SV40 large T (ref. 6) (a gift from B. Viollet) were plated in 6-cm plates 1 day before transfection with 500 pmol of siRNA using Lipofectamine 2000 (Invitrogen). At 48 h after transfection, the cells were replated in six-well plates for western blot analysis or in 12-well plates for measurements of cell death and reactive oxygen species. The infections with lentiviruses and retroviruses were conducted overnight, and infected cells were selected with blasticidin, puromycin or hygromycin under the following conditions: 25 μg ml^{-1} blasticidin for 6 days or 0.5 μg ml^{-1} puromycin for 3 days for A549 cells; 10 μg ml^{-1} blasticidin for 4 days for HeLa cells; 15 μg ml^{-1} blasticidin for 4 days or 1 μg ml^{-1} puromycin for 4 days for H1703 cells; 10 μg ml^{-1} blasticidin for 4 days or 1 μg ml^{-1} puromycin for 4 days for MCF7 cells; 10 μg ml^{-1} blasticidin for 4 days or 100 μg ml^{-1} hygromycin for 6 days for MEF-AMPKα-KO. For the western blot analyses, protein extracts were prepared in lysis buffer, as described previously[27].

Reagents and antibodies

5-Thio-D-glucose was purchased from ICN Biomedical. DCF and DHE were purchased from Molecular Probes. [^{3}H]Acetate, [9,10-^{3}H]palmitate and 2-deoxy[^{3}H]glucose were obtained from PerkinElmer. STO-609 and Ku-55933 were purchased from Calbiochem. All other chemicals were purchased from Sigma-Aldrich unless otherwise indicated. Antibodies against LKB1, AMPKα1/2, ACC, P-ACC and HK2 were purchased from Cell Signaling, and antibodies specific for ACC2, catalase and α-tubulin were purchased from Sigma-Aldrich. The G6PD antibody was purchased from Bethyl Lab, and the GSK3 antibody was from QCB.

Plasmids, RNA-mediated interference (RNAi) and viruses

The complementary DNAs encoding ACC1 and ACC2 were provided by M. R. Montminy. Site-directed mutagenesis of ACC1 (S79A) and ACC2 (S212) was performed with the QuickChange II XL Kit (Stratagene), as recommended by the manufacturer. The mutants were subcloned into the pLent6-D-TOPO vector (Invitrogen). SMART-pool siRNAs targeting human ACC1 and ACC2 and mouse ACC1 and ACC2 were purchased from Dharmacon (hACC1: 5′-gatgtgagcctgcggaata-3′, 5′-ccacttggctgagcgattg-3′, 5′-gcaattagattcgttgtca-3′, 5′-gatcttagcggaccaatat-3′, hACC2: 5′-gatacatgatcacggatat-3′, 5′-gaagagaggtctacacatc-3′, 5′-aggaagaggttgacagtta-3′, 5′-cctcgtagatgtggaatta-3′, mACC1: 5′-caagactgatggcgatatt-3′, 5′-gaaaatagactcacaacga-3′, 5′-ggaagttaatccagtatat-3′, 5′-tcaatgtgatgaatggata-3′, mACC2: 5′-gtggtgacgggacgagcaa-3′, 5′-gagattaagttccggaaga-3′, 5′-tcaattatctgaagcggga-3′, 5′-gaagagaggtctacacgtc-3′). The constructs (pENTR-U6) expressing an shRNA targeting LacZ, G6PD, ACC1 or ACC2 were generated with the BLOCK-iT U6 RNAi Entry Vector Kit (Invitrogen). The shRNA sequences used were 5′-GCCTCAGTGCCACTTGACA-3′ for hG6PD[28], 5′-TACAAGGGATACAGGTATTTA-3′ for hACC1 2, 5′-GTGGAGCTGATTGTGGACATT-3′ for hACC2 1, 5′-GACGGCCTTAGACAATACAAA-3′ for hACC2 2, 5′-GCAGATTGCCAACATCCTAGA-3′ for mouse ACC1, and 5′-GTGGTGACGGGACGAGCAA-3′ for mouse ACC2. The shRNA expression cassettes were transferred to a lentiviral vector (plenti6) with the use of the BLOCK-iT Lentiviral RNAi Expression System (Invitrogen). The lentiviral constructs (pLKO.1) expressing shRNAs for a non-targeted control (5′-CAACAAGATGAAGAGCACCAA-3′) and hLKB1 (5′-GCCAACGTGAAGAAGGAAATT-3′) were purchased from Sigma-Aldrich. The lentiviral vector expressing the AMPKα1-specific shRNA with the sequence 5′-CTATGCTGCACCAGAAGTA-3′ was a gift from M. Karin, and was described previously[29]. All lentiviruses were produced with the BLOCK-iT Lentiviral RNAi Expression System (Invitrogen), as recommended by the manufacturer. To produce retroviruses expressing dominant-negative p53 (p53-DN) or constitutively active Ras (Ras^{V12}), the pBabe-Puro-GSE56 plasmid or the pBabe-hygro-Ras^{V12} plasmid was transfected into amphotropic or ecotropic Phoenix cells, respectively, as described previously[30].

Cell death assay

In most of the experiments, apoptotic cell death was measured by using DAPI staining, as described previously[27,31]. Cells were plated at a low density ($(0.7–1) \times 10^5$ cells per well in a 12-well plate); on the next day, the cells were washed with PBS and cultured in glucose-free medium supplemented with dialysed FBS. At each time point, the cells were fixed by the direct addition of formaldehyde (final concentration 12%) to the culture medium. After overnight fixation, the cells were stained for 5 min with DAPI (1 μg ml^{-1}), and then left in PBS. The cells were detected with fluorescence microscopy, and cells with condensed and/or fragmented chromatin indicative of apoptosis were counted as dead cells. For MCF7 cells, a trypan blue exclusion assay was performed to measure cell death.

Assays of reactive oxygen species

The intracellular levels of H_2O_2 and O_2^- were measured with DCF and DHE, respectively. Cells (10^5) were plated in a 12-well plate and treated with DCF or DHE for 30 min. The cells were then washed with PBS and collected as single-cell suspensions. Fluorescence was detected by flow cytometry.

NADPH, GSH and ATP assays

The intracellular levels of NADPH and total NADP (NADPH+$NADP^+$) were measured with previously described enzymatic cycling methods, with modifications[32,33]. In brief, 1.8×10^6 cells were plated in 10-cm dishes; on the next day, the cells were lysed in 400 μl of extraction buffer (20 mM nicotinamide, 20 mM $NaHCO_3$, 100 mM Na_2CO_3) and centrifuged. For NADPH extraction, 150 μl of the supernatant was incubated at 60 °C for 30 min. Next, 160 μl of NADP-cycling buffer (100 mM Tris-HCl pH 8.0, 0.5 mM thiazolyl blue, 2 mM phenazine ethosulfate, 5 mM EDTA) containing 1.3U of G6PD was added to a 96-well plate containing 20 μl of the cell extract. After a 1-min incubation in the dark at 30 °C, 20 μl of 10 mM glucose 6-phosphate (G6P) was added to the mixture, and the change in absorbance at 570 nm was measured every 30 s for 4 min at 30 °C with a microplate reader. The concentration of $NADP^+$ was calculated by subtracting[NADPH] from [total NADP]. The intracellular levels of GSH and total glutathione (GSSG + GSH) were measured with the use of enzymatic cycling methods, as described previously[34]. The intracellular level of ATP was measured with an ATPlite assay kit (Perkin Elmer).

Metabolism assays

Fatty-acid synthesis and oxidation were measured as described previously[35,36]. In brief, 10^5 cells were seeded in a 12-well plate for 1 day. For the glucose starvation experiments, the cells were incubated in glucose-free medium for 2 h, and either [^{3}H]acetate (for FAS) or [9,10-^{3}H]palmitate (for FAO) was added for a further 3 h. For matrix detachment, 10^5 cells were seeded on poly-HEMA-coated 12-well plates for 2 h, and either [^{3}H]acetate or [9,10-^{3}H]palmitate was added for a further 3 h. For the measurement of FAS, total lipids were extracted from [^{3}H]acetate-treated cells with chloroform/methanol. For the measurement of FAO, the medium from [9,10-^{3}H]palmitate-treated cells was collected to recover ^3H_2O using Dowex 1X8-200 columns. ^{3}H-labelled lipids and water were quantified by liquid scintillation counting. Glucose uptake was measured with 2-deoxy[^{3}H]glucose.

Soft-agar assay

A total of 3×10^4 cells were suspended in DMEM (10% FBS, 5 mM glucose) containing 0.35% agarose and layered on solidified medium containing 0.7% agarose in six-well plates. For MCF7 cells, 1 mM sodium pyruvate was added to the medium. After solidification, the top layer was covered with the medium. When necessary, 2 mM NAC or 5 μg ml^{-1} STO-609 was added to each layer and the cover medium. The medium was replaced every week. Images were taken after 3–4 weeks and analysed with ImageJ software.

Xenograft assay

Male and female athymic nude mice (6–8 weeks old) were purchased from Charles River Laboratories. A549 cells (2×10^6 per 0.1 ml of PBS) or AMPKα-KO-MEFs-Ras^{V12} cells (5×10^6 per 0.1 ml of PBS) expressing the LacZ-specific, ACC1-specific or ACC2-specific shRNA were injected subcutaneously into both the left and right flanks of each mouse. A xenograft assay using A549 cells was performed twice. MCF7 cells were injected orthotopically into the mammary fat pads (two positions per mouse) in two different conditions, namely the absence (Supplementary Fig. 25) and presence (Fig. 4g) of 10% Matrigel in cell suspensions. Before injection, 17β-oestradiol pellets (1.7 mg/pelleted, 60-day release; Innovative Research of America) were implanted in each mouse. The tumour size was measured every week, and the tumour volume was calculated with the equation V (in mm^3) = $a \times b^2/2$, where a is the longest diameter and b is the shortest diameter. When the tumour size reached the end-point criterion (a diameter greater than 2 cm), the mouse was killed. All animal experiments were performed in accordance with the animal care policies

of the University of Illinois at Chicago and were approved by the Animal Care Committee of the University of Illinois at Chicago.

Statistical analysis

All statistical analysis was performed with unpaired two-tailed Student's *t*-tests, and all data are expressed as means and s.e.m. for at least three independent experiments, unless otherwise indicated.

Supplementary Material

Refer to Web version on PubMed Central for supplementary material.

Acknowledgments

We thank B. Viollet for the AMPK-KO MEFs, M. R. Montminy for the ACC complementary DNA, and G. Hatzivassiliou for comments on the manuscript. This work was supported by grants CA090764, AG016927 and AG025953 from the National Institutes of Health, by the Chicago Biomedical Consortium with support from The Searle Funds at The Chicago Community, and by grant P60DK20595 to the Diabetes Research and Training Center, University of Chicago (to N.H.).

References

1. Folkman J. Angiogenesis and apoptosis. Semin. Cancer Biol. 2003; 13:159–167. [PubMed: 12654259]
2. Jones RG, Thompson CB. Tumor suppressors and cell metabolism: a recipe for cancer growth. Genes Dev. 2009; 23:537–548. [PubMed: 19270154]
3. Shackelford DB, Shaw RJ. The LKB1–AMPK pathway: metabolism and growth control in tumour suppression. Nature Rev. Cancer. 2009; 9:563–575. [PubMed: 19629071]
4. Bardeesy N, et al. Loss of the Lkb1 tumour suppressor provokes intestinal polyposis but resistance to transformation. Nature. 2002; 419:162–167. [PubMed: 12226664]
5. Kato K, et al. Critical roles of AMP-activated protein kinase in constitutive tolerance of cancer cells to nutrient deprivation and tumor formation. Oncogene. 2002; 21:6082–6090. [PubMed: 12203120]
6. Laderoute KR, et al. 5′-AMP-activated protein kinase (AMPK) is induced by low-oxygen and glucose deprivation conditions found in solid-tumor microenvironments. Mol. Cell. Biol. 2006; 26:5336–5347. [PubMed: 16809770]
7. Chhipa RR, Wu Y, Mohler JL, Ip C. Survival advantage of AMPK activation to androgen-independent prostate cancer cells during energy stress. Cell. Signal. 2010; 22:1554–1561. [PubMed: 20570728]
8. Corradetti MN, Inoki K, Bardeesy N, DePinho RA, Guan KL. Regulation of the TSC pathway by LKB1: evidence of a molecular link between tuberous sclerosis complex and Peutz–Jeghers syndrome. Genes Dev. 2004; 18:1533–1538. 10.1101/gad.1199104. [PubMed: 15231735]
9. Shaw RJ, et al. The tumor suppressor LKB1 kinase directly activates AMP-activated kinase and regulates apoptosis in response to energy stress. Proc. Natl Acad. Sci. USA. 2004; 101:3329–3335. [PubMed: 14985505]
10. Jones RG, et al. AMP-activated protein kinase induces a p53-dependent metabolic checkpoint. Mol. Cell. 2005; 18:283–293. [PubMed: 15866171]
11. Le Goffe C, et al. Metabolic control of resistance of human epithelial cells to H_2O_2 and NO stresses. Biochem. J. 2002; 364:349–359. [PubMed: 12023877]
12. Hardie DG, Pan DA. Regulation of fatty acid synthesis and oxidation by the AMP-activated protein kinase. Biochem. Soc. Trans. 2002; 30:1064–1070. [PubMed: 12440973]
13. Abu-Elheiga L, Matzuk MM, Abo-Hashema KA, Wakil SJ. Continuous fatty acid oxidation and reduced fat storage in mice lacking acetyl-CoA carboxylase 2. Science. 2001; 291:2613–2616. [PubMed: 11283375]

14. Zhou W, et al. Fatty acid synthase inhibition triggers apoptosis during S phase in human cancer cells. Cancer Res. 2003; 63:7330–7337. [PubMed: 14612531]
15. Canto C, et al. AMPK regulates energy expenditure by modulating NAD^+ metabolism and SIRT1 activity. Nature. 2009; 458:1056–1060. [PubMed: 19262508]
16. Schafer ZT, et al. Antioxidant and oncogene rescue of metabolic defects caused by loss of matrix attachment. Nature. 2009; 461:109–113. [PubMed: 19693011]
17. Jang T, et al. 5′-AMP-activated protein kinase activity is elevated early during primary brain tumor development in the rat. Int. J. Cancer. 2011; 128:2230–2239. [PubMed: 20635388]
18. Kim HS, et al. Microarray analysis of papillary thyroid cancers in Korean. Korean J. Intern. Med. 2010; 25:399–407. [PubMed: 21179278]
19. Zaugg K, et al. Carnitine palmitoyltransferase 1C promotes cell survival and tumor growth under conditions of metabolic stress. Genes Dev. 2011; 25:1041–1051. [PubMed: 21576264]
20. Hatzivassiliou G, et al. ATP citrate lyase inhibition can suppress tumor cell growth. Cancer Cell. 2005; 8:311–321. [PubMed: 16226706]
21. Migita T, et al. Fatty acid synthase: a metabolic enzyme and candidate oncogene in prostate cancer. J. Natl. Cancer Inst. 2009; 101:519–532. [PubMed: 19318631]
22. Knowles LM, Yang C, Osterman A, Smith JW. Inhibition of fatty-acid synthase induces caspase-8-mediated tumor cell apoptosis by up-regulating DDIT4. J. Biol. Chem. 2008; 283:31378–31384. [PubMed: 18796435]
23. Bandyopadhyay S, et al. Mechanism of apoptosis induced by the inhibition of fatty acid synthase in breast cancer cells. Cancer Res. 2006; 66:5934–5940. [PubMed: 16740734]
24. Wellen KE, et al. ATP-citrate lyase links cellular metabolism to histone acetylation. Science. 2009; 324:1076–1080. [PubMed: 19461003]
25. Migita T, et al. ATP citrate lyase: activation and therapeutic implications in non-small cell lung cancer. Cancer Res. 2008; 68:8547–8554. [PubMed: 18922930]
26. Ji H, et al. LKB1 modulates lung cancer differentiation and metastasis. Nature. 2007; 448:807–810. [PubMed: 17676035]
27. Bhaskar PT, et al. mTORC1 hyperactivity inhibits serum deprivation-induced apoptosis via increased hexokinase II and GLUT1 expression, sustained Mcl-1 expression, and glycogen synthase kinase 3β inhibition. Mol. Cell. Biol. 2009; 29:5136–5147. [PubMed: 19620286]
28. Li D, et al. A new G6PD knockdown tumor-cell line with reduced proliferation and increased susceptibility to oxidative stress. Cancer Biother. Radiopharm. 2009; 24:81–90. [PubMed: 19243250]
29. Budanov AV, Karin M. p53 target genes sestrin1 and sestrin2 connect genotoxic stress and mTOR signaling. Cell. 2008; 134:451–460. 10.1016/j.cell.2008.06.028. [PubMed: 18692468]
30. Skeen JE, et al. Akt deficiency impairs normal cell proliferation and suppresses oncogenesis in a p53-independent and mTORC1-dependent manner. Cancer Cell. 2006; 10:269–280. [PubMed: 17045205]
31. Kennedy SG, et al. The PI 3-kinase/Akt signaling pathway delivers an anti-apoptotic signal. Genes Dev. 1997; 11:701–713. [PubMed: 9087425]
32. Wagner TC, Scott MD. Single extraction method for the spectrophotometric quantification of oxidized and reduced pyridine nucleotides in erythrocytes. Anal. Biochem. 1994; 222:417–426. [PubMed: 7864367]
33. Zerez CR, Lee SJ, Tanaka KR. Spectrophotometric determination of oxidized and reduced pyridine nucleotides in erythrocytes using a single extraction procedure. Anal. Biochem. 1987; 164:367–373. [PubMed: 3674385]
34. Rahman I, Kode A, Biswas SK. Assay for quantitative determination of glutathione and glutathione disulfide levels using enzymatic recycling method. Nature Protocols. 2006; 1:3159–3165.
35. Buzzai M, et al. The glucose dependence of Akt-transformed cells can be reversed by pharmacologic activation of fatty acid beta-oxidation. Oncogene. 2005; 24:4165–4173. [PubMed: 15806154]

36. Deberardinis RJ, Lum JJ, Thompson CB. Phosphatidylinositol 3-kinase-dependent modulation of carnitine palmitoyltransferase 1A expression regulates lipid metabolism during hematopoietic cell growth. J. Biol. Chem. 2006; 281:37372–37380. [PubMed: 17030509]

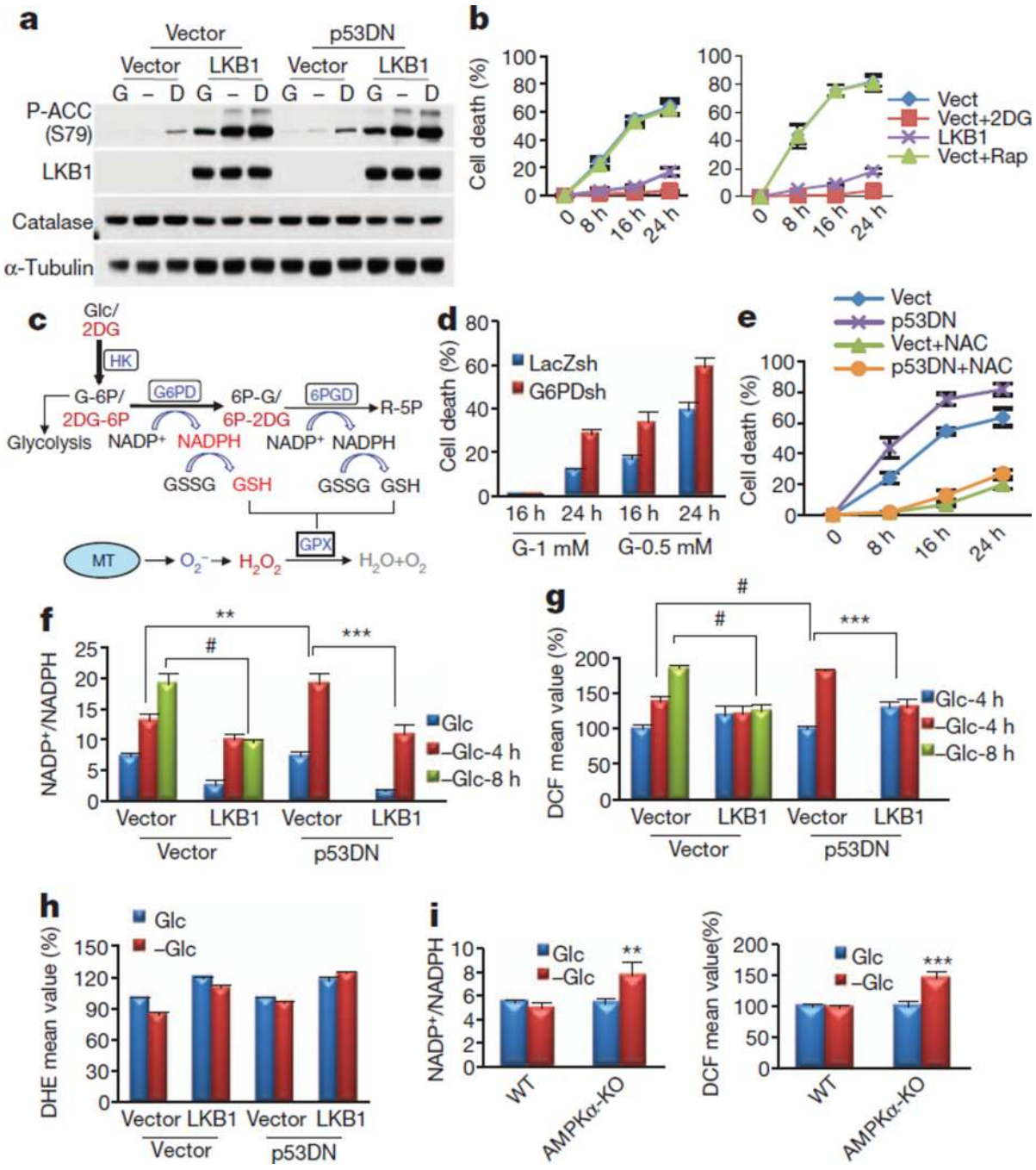

Figure 1. The failure to activate AMPK accelerates NADPH depletion, oxidative stress and cell death in the absence of glucose

a, Immunoblotting analyses after incubating A549 cells expressing empty vector, LKB1, p53DN or both p53DN and LKB1 in the absence (−) or presence of 5mMglucose (G) or 2DG (D) for 2 h. **b**, Cell death quantification after glucose starvation. For A549-Vect (left) and A549-p53DN (right) cells, 5 mM 2DG (Vect+2DG) or 100 nM rapamycin (Vect+Rap) were added to the medium. **c**, Illustration depicting partial metabolism of 2DG through the PPP, which could generate NADPH/GSH and eliminate H_2O_2 generated from mitochondria (MT) (see the text for details). Glc, glucose; HK, hexokinase; G-6P, glucose 6-phosphate; 6PGD, 6-phosphogluconate dehydrogenase; 2DG-6P, 2-deoxyglucose 6-phosphate; 6P-G, 6-

phosphogluconate; 6P-2DG, 6-phospho 2-deoxygluconate; R-5P, ribulose 5-phosphate. **d**, Quantification of cell death of A549 cells expressing LacZ-shRNA or G6PD-shRNA cultured in 1 mM or 0.5 mM glucose. **e**, Cell death quantification at different time points after glucose depletion in the presence or absence of 2 mM NAC. **f, g**, $NADP^+$/NADPH ratio (**f**) and H_2O_2 level (**g**) after incubation in the absence (−Glc) or presence of 5 mM glucose (Glc) for 4 or 8 h. **h**, O_2^- levels after incubation in the absence or presence of 5 mM glucose for 4 h. **i**, $NADP^+$/NADPH ratio (left) and H_2O_2 level (right) in wild-type (WT) or AMPKα-KO MEFs cultured in glucose-free medium in the absence (−Glc) or presence of 5 mM glucose (Glc) for 5 h. Results in **g, h** and **i** (right) are expressed as the percentage change in the mean DCF/DHE values relative to the glucose-treated control. Results are shown as means and s.e.m. for three independent (**b, d, f, h, i**) or four (**e, g**) experiments. Asterisk, $P < 0.05$; two asterisks, $P < 0.01$; three asterisks, $P < 0.005$; hash, $P < 0.001$ versus the glucose-treated control in each group.

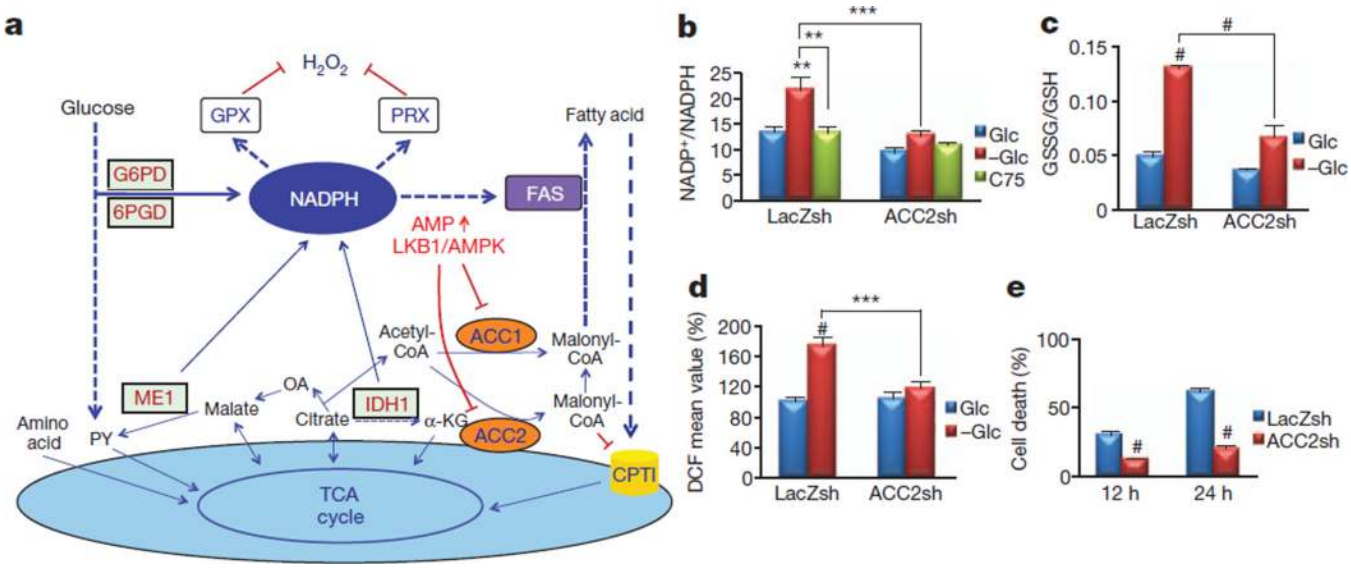

Figure 2. ACC2 ablation recapitulates AMPK activation, maintaining the NADPH level and decreasing the H_2O_2 level during glucose deprivation

a, A schematic illustration depicting one potential mechanism by which AMPK regulates NADPH homeostasis (see the text for details). PY, pyruvate; OA, oxaloacetate; α-KG, α-oxoglutarate; ME, malic enzyme; IDH, isocitrate dehydrogenase; TCA, tricarboxylic acid. **b–d**, A549 cells expressing LacZ-shRNA or ACC2-shRNA 2 were incubated in glucose-free medium in the absence (–Glc) or presence of 5 mM glucose (Glc) or with 20 μg ml^{-1} C75. After 6 h, the $NADP^+$/NADPH ratio (**b**), GSSG/GSH ratio (**c**) and H_2O_2 level (**d**) were measured. **e**, Quantification of cell death after glucose starvation for 10 and 24 h. Results in **d** are expressed as the percentage change in the mean DCF values relative to the glucose-treated control. Results are shown as means and s.e.m. for three independent experiments. Two asterisks, $P < 0.01$; three asterisks, $P < 0.005$; hash, $P < 0.001$ versus the glucose-treated control in each group (**b–d**) or versus the LacZsh control (**e**) at each time point.

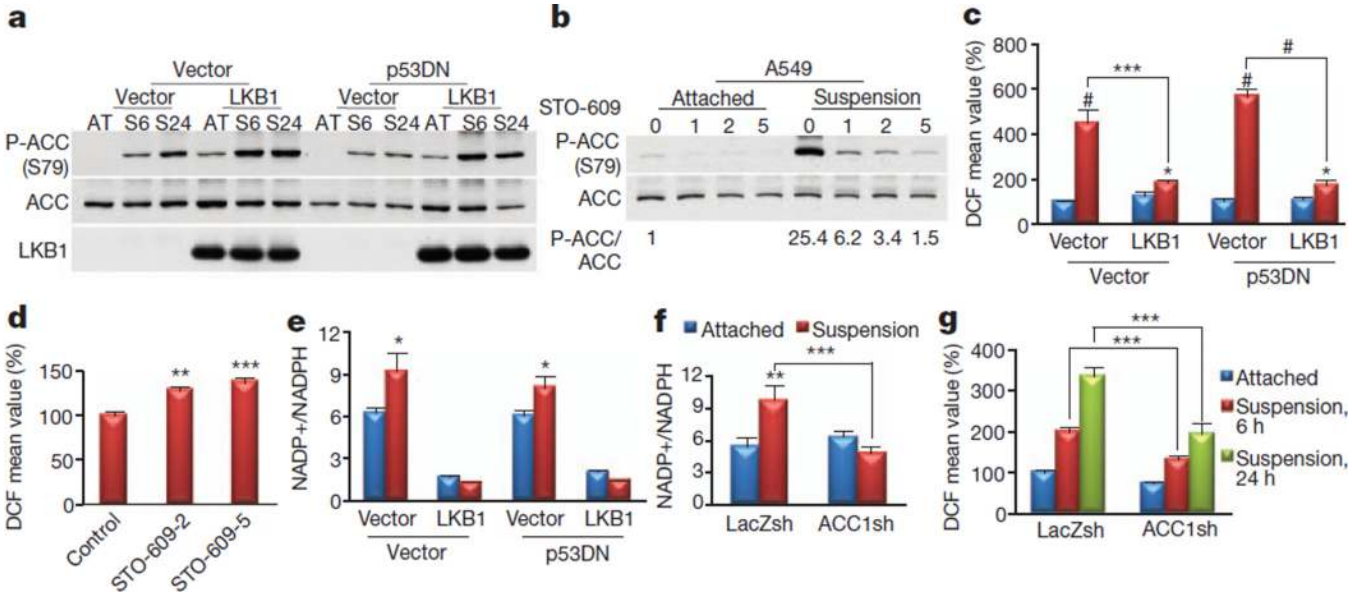

Figure 3. AMPK-mediated inhibition of ACC1 is required to maintain the NADPH and reactive oxygen species levels after matrix detachment

a, A549-Vect-Vect, A549-Vect-LKB1, A549-p53DN-Vect and A549-p53DN-LKB1 cells were grown attached (AT) or in suspension (S6, S24) and subjected to immunoblotting at the indicated time points (6 and 24 h). **b**, A549 cells were grown attached or in suspension in the presence or absence of STO-609 (1, 2 or 5 μg ml^{-1}) for 6 h and subjected to immunoblotting for quantification of phospho-ACC (P-ACC). **c, d**, H_2O_2 levels after growth attached (blue columns) or in suspension (red columns) for 24 h (**c**) or for 6 h in the presence or absence of 2 or 5 μg ml^{-1} STO-609 (**d**). **e**, $NADP^+$/NADPH ratio after growth attached (blue columns) or in suspension (red columns) for 24 h. **f, g**, The effect of ACC knockdown on $NADP^+$/NADPH ratio (**f**) or H_2O_2 level (**g**) after in suspension for 24 h (**f**) or for 6 and 24 h (**g**). Results in **c, d** and **g** are expressed as the percentage change in the mean DCF values over the values of the attached control. Results are shown as means and s.e.m. for three independent experiments. Asterisk, $P < 0.05$; two asterisks, $P < 0.01$; three asterisks, $P < 0.005$; hash, $P < 0.001$ versus the attached condition in each group (**c, e–g**) or versus the control (**d**).

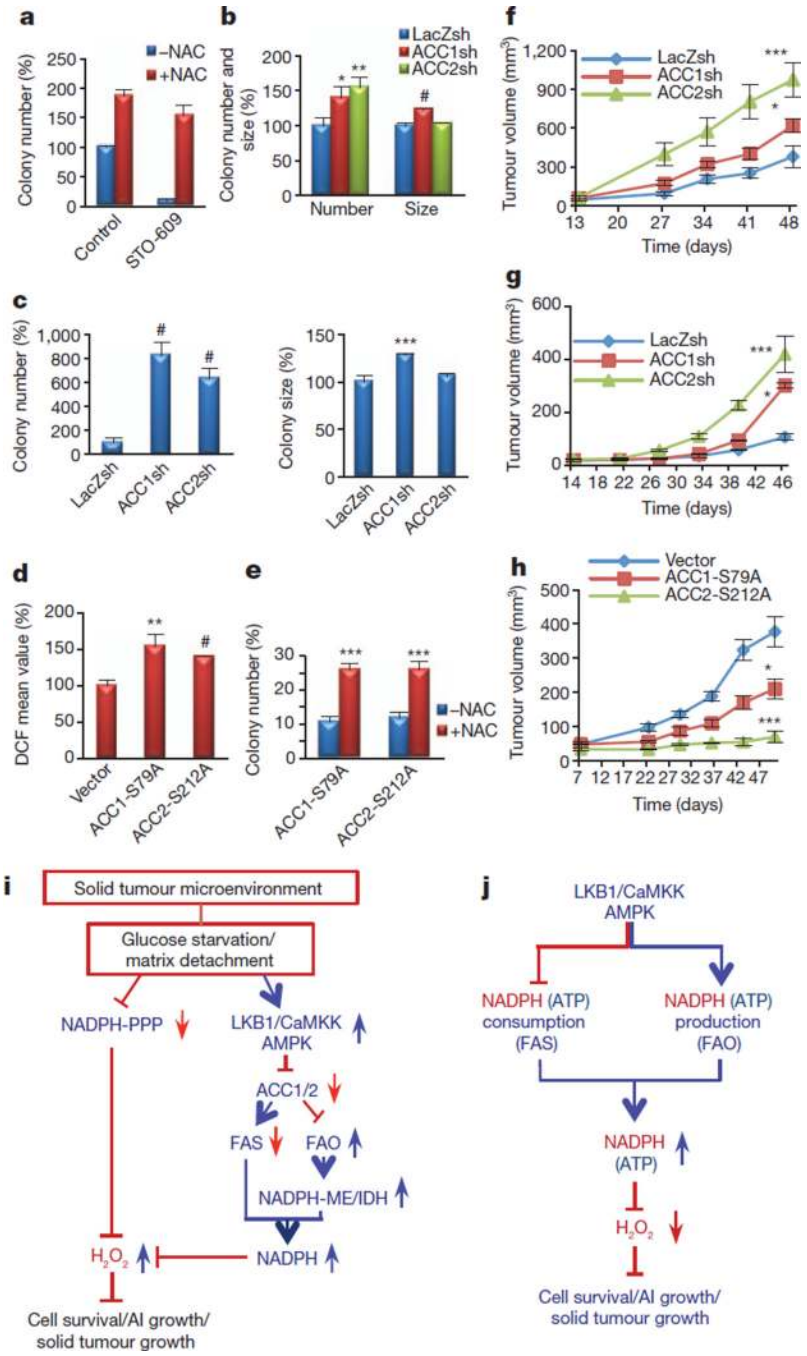

Figure 4. AMPK-mediated inhibition of ACC1 or ACC2 promotes anchorage-independent growth and solid tumour formation *in vivo*

a, Quantification of soft agar colonies of A549 cells in the presence or absence of 5 μg ml^{-1} STO-609, with or without 2 mM NAC. **b, c**, A549 cells (**b**) or AMPKα-KO-Ras^{V12}-MEFs (**c**) expressing LacZ-shRNA, ACC1-shRNA, or ACC2-shRNA were plated on soft agar, and the number and size of the colonies were analysed. Results are expressed as the percentage change in the colony number and size relative to the –NAC control (**a**) or the LacZsh control (**b, c**). **d, e**, MCF7 cells expressing ACC1-S79A or ACC2-S212A were generated and grown in suspension for 6 h before quantification of the H_2O_2 level (**d**) or were subjected to soft agar assay (with or without 2 mM NAC) (**e**). Results are expressed as the percentage change

in the mean DCF values (**d**) or colony number (**e**) over the values of the vector control. Results are expressed as means and s.e.m. for three independent experiments. **f, g**, A549 cells (**f**), or AMPKα-KO-Ras^{V12} cells (**g**) expressing LacZ-shRNA, ACC1-shRNA, or ACC2-shRNA were injected subcutaneously into nude mice. **h**, MCF7 cells expressing vector, ACC1-S79A or ACC2-S212A were mixed with Matrigel (10%) and injected orthotopically into the mammary fat pads of nude mice. Tumour growth was monitored and measured weekly. Results are shown as means and s.e.m. for four mice in each group. Asterisk, $P < 0.05$; two asterisks, $P < 0.01$; three asterisks, $P < 0.005$; hash, $P < 0.001$ versus LacZsh (**b, c**), vector (**d**) or −NAC in each group (**e**), and versus LacZ-shRNA (**f, g**) or vector (**h**) at each time point. **i**, Summary: under energy stress when PPP is impaired, AMPK activation attenuates cell death by maintaining NADPH level through FAO-induced NADPH production and by inhibiting NADPH consumption in FAS. AI growth, anchorage-independent growth. **j**, Proposed model: in addition to its function in ATP homeostasis, the LKB1/CaMKK–AMPK/ACC1/2 axis has a key function in NADPH homeostasis to decrease H_2O_2 level and to promote cancer cell survival and metabolic adaptation.